Title

Olfactory ensheathing cell–neurite alignment enhances neurite outgrowth in scar-like cultures

Authors

Khankan, Rana R
Wanner, Ina B
Phelps, Patricia E

Publication Date

2015-07-01

DOI

10.1016/j.expneurol.2015.03.025

Peer reviewed

Published in final edited form as:

Exp Neurol. 2015 July ; 269: 93–101. doi:10.1016/j.expneurol.2015.03.025.

Olfactory ensheathing cell-neurite alignment enhances neurite outgrowth in scar-like cultures

Rana R. Khankan[1], **Ina B. Wanner**[2], and **Patricia E. Phelps**[1]

Rana R. Khankan: khankan@ucla.edu; Ina B. Wanner: IWanner@mednet.ucla.edu; Patricia E. Phelps: pphelps@physci.ucla.edu

[1]Department of Integrative Biology and Physiology, UCLA, Los Angeles, CA 90095

[2]Department of Psychiatry and Biobehavioral Science, UCLA, Los Angeles, CA 90095

Abstract

The regenerative capacity of the adult CNS neurons after injury is strongly inhibited by the spinal cord lesion site environment that is composed primarily of the reactive astroglial scar and invading meningeal fibroblasts. Olfactory ensheathing cell (OEC) transplantation facilitates neuronal survival and functional recovery after a complete spinal cord transection, yet the mechanisms by which this recovery occurs remain unclear. We used a unique multicellular scar-like culture model to test if OECs promote neurite outgrowth in growth inhibitory areas. Astrocytes were mechanically injured and challenged by meningeal fibroblasts to produce key inhibitory elements of a spinal cord lesion. Neurite outgrowth of postnatal cerebral cortical neurons was assessed on three substrates: quiescent astrocyte control cultures, reactive astrocyte scar-like cultures, and scar-like cultures with OECs. Initial results showed that OECs enhanced total neurite outgrowth of cortical neurons in a scar-like environment by 60%. We then asked if the neurite growth-promoting properties of OECs depended on direct alignment between neuronal and OEC processes. Neurites that aligned with OECs were nearly three times longer when they grew on inhibitory meningeal fibroblast areas and twice as long on reactive astrocyte zones compared to neurites not associated with OECs. Our results show that OECs can independently enhance neurite elongation and that direct OEC-neurite cell contact can provide a permissive substrate that overcomes the inhibitory nature of the reactive astrocyte scar border and the fibroblast-rich spinal cord lesion core.

Please address correspondence to: Patricia E. Phelps, Ph.D., Dept. of Integrative Biology and Physiology, UCLA, Terasaki Life Sciences Building, 610 Charles Young Dr. East, Los Angeles, CA 90095-7239, Fax: (310) 206-9184, Telephone: (310) 825-7264, pphelps@physci.ucla.edu.

Conflict of interest statement:
None

Keywords

Spinal cord injury; Reactive astrocytes; OEC; Cell adhesion; Astrocytes; Meningeal fibroblasts; Neurite outgrowth

Introduction

Olfactory receptor neurons are generated and then project their axons from the peripheral into the central nervous system throughout life (CNS; Graziadei and Monti Graziadei, 1985). The regenerative ability of the olfactory receptor neurons is enhanced by olfactory ensheathing cells (OECs), a distinct glia with features of both Schwann cells and astrocytes (Doucette, 1991; Ramón-Cueto and Valverde, 1995). After an olfactory nerve injury, OECs survive and maintain a conduit so that newly generated axons can grow into the damaged inhibitory areas of the adult olfactory system, cross the glia limitans, and contact their olfactory bulb targets (Doucette, 1991; Li et al., 2005). Due to these attributes, OECs are considered a promising treatment following spinal cord injury (SCI; Lu et al., 2002; Lopez-Vales et al., 2006; Kubasak et al,. 2008; Ramón-Cueto et al., 1998, 2000; Tabakow et al., 2014; Takeoka et al., 2011; Ziegler et al., 2011).

While adult CNS neurons have a capacity to regenerate, they usually fail to regrow functional axons due to a non-permissive or inhibitory environment. After injury astrocytic cell bodies hypertrophy and their processes widen, cluster together, elongate, and display increased glial fibrillary acidic protein (GFAP) immunoreactivity, a response defined as reactive astrogliosis (Barrett et al., 1981; Reier and Houle, 1988; Silver and Miller, 2004; Sofroniew, 2009). A GFAP-positive scar border of reactive astrocytes forms due to both the injury and the invasion of meningeal fibroblasts (Silver and Miller, 2004; Wanner et al., 2013). The processes of newly generated reactive astrocytes become oriented transversely to isolate the intact spinal cord from the lesion core, a response that limits axon regeneration (Barnabé-Heider et al., 2010; Li et al., 2012; Wanner et al., 2013). Additionally, increased chondroitin sulfate proteoglycan (CSPG) and class 3 semaphorin (Sema3) expression contribute to the inhibitory environment formed at the lesion site (Buss et al., 2009; Fitch and Silver, 2008; Hu et al., 2010; Pasterkamp et al., 2001). A scar-like culture model (Wanner et al., 2008) replicates the wide-spread reduction of neurite outgrowth as a result of reactive astrogliosis and elevation of inhibitory CSPGs phosphacan, neurocan, and tenascin. The scar-like environment in this model is generated by the addition of two injury-inducing factors to quiescent astrocytes: 1) confrontation with meningeal fibroblasts and 2) mechanical stretch (Wanner et al., 2008).

OECs may overcome the injury site inhibition and promote neurite sprouting and outgrowth by providing both an adhesive cellular substrate and permissive soluble factors (Chung et al., 2004; Kafitz and Greer 1999; Pellitteri et al., 2009; Sonigra et al., 1999). Indeed OECs express multiple adhesion molecules involved in axon outgrowth, secrete trophic factors, and ensheath growing axons to protect them from inhibitory molecules (Doucette, 1990; Lipson et al., 2003; Ramón-Cueto and Valverde, 1995; Woodhall et al., 2001). Trophic factors, such as brain-derived neurotrophic factor (BDNF), contribute to the ability of OECs

to enhance axon regeneration on an inhibitory substrate (Ruitenberg et al., 2003; Runyan and Phelps, 2009), but the contact-mediated OEC-neuron interactions are not well studied.

The growth-promoting characteristics of OECs lead to their use as therapeutic cellular grafts following SCI. Over the past decade a number of studies reported that OECs support axon regeneration *in vivo*, even after a complete transection (Kubasak et al, 2008; Lopez-Vales et al., 2006; Lu et al., 2002; Ramón-Cueto et al., 1998, 2000; Tabakow et al., 2014; Takeoka et al., 2011; Ziegler et al., 2011). Despite the reported functional improvements, most of these studies could not identify OECs post-implantation and consequently the OEC interactions in a SCI environment remain unclear. In the present study, we used an established model of SCI that recapitulates the inhibitory environment of the astroglial scar and its fibroblast border (Wanner et al., 2008) to test how OEC transplantation facilitates neurite regeneration. We identified OEC-neurite alignment as a critical regulator of neurite outgrowth on the growth-inhibitory substrates in scar-like cultures.

Materials and Methods

Astrocyte-meningeal fibroblast co-culture

Methods to prepare co-cultures of astrocytes and meningeal cells (predominantly fibroblasts, but also microglia and blood vessels) were similar to those reported in Wanner et al. (2008, 2012). Astrocytes were cultured from neonatal rat cerebral cortices in 5% fetal bovine serum (FBS, Hyclone, Logan, UT) and upon reaching confluency, cultures were switched to a mixture of 1:1 DMEM and Ham's F12 (D/F medium, Gibco) supplemented with 5% horse serum. Approximately 200,000 astrocytes were seeded onto deformable membranes (962 mm^2 Bioflex 6 well plates, Flexcell Int. Corp., Hillsborough, NC) previously coated with collagen (Fig. 1; control culture). Astrocyte cultures were slowly withdrawn from serum and kept serum-free until the addition of meningeal cells.

Meningeal fibroblasts were isolated from newborn rat cortical meninges, dissociated and resuspended with 3% trypsin, collagenase, and DNAse I. They were grown for 5 days on poly-L-lysine-coated dishes (PLL; Sigma, St. Louis, MO). Meningeal fibroblasts were added to the astrocytes on deformable membranes after 4 weeks *in vitro* with 130,000 cells per culture in 10% FBS/DF medium (Fig. 1). Astrocyte-fibroblast co-cultures grown on deformable membranes were given two short pressure pulses (3.5–3.8 psi) with a pressure controller (Ellis et al., 1995) that induced abrupt membrane deformation and mechanical trauma to the cells (Fig. 1; scar-like culture).

OEC primary culture

Olfactory bulbs were collected from 8–10 weeks old Sprague Dawley rats and the leptomeninges were removed to reduce fibroblast contamination. Methods to prepare OEC primary cultures were adopted from Ramón-Cueto et al. (2000). OECs were dissected from the first two layers of the olfactory bulb and washed in Hank's Balanced Salt Solution (HBSS, Gibco, Rockville, MD) prior to tissue centrifugation at 365 g for 5 min. The tissue pellet was first resuspended in 0.1% trypsin and HBSS without Ca^{2+}/Mg^{2+} (Gibco), then placed in a 37°C water bath, and mixed intermittently for 10 min. D/F medium

supplemented with 10% FBS and 1% Penicillin/Streptomycin (P/S, Gibco) was used to inactivate trypsin prior to centrifugation. Dissociated cells were rinsed and centrifuged 3 times, and then plated into 25 cm^2 culture flasks pre-coated with 0.5 mg/ml PLL. Cells were maintained at 37°C for 7 days and D/F medium was changed every 2 days.

OEC immunopurification

Hydrophobic petri dishes were coated overnight with Biotin-SP-conjugated AffiniPure goat anti-mouse IgG (1:1000; Jackson Immunoresearch Laboratories, West Grove, PA) in 50 mM Tris buffer. Dishes were washed 4 times with 25mM PBS (Gibco) and then incubated overnight with antibody against p75-nerve growth factor receptor (anti-p75-NGFR, 1:5; clone 192, Chandler et al., 1984) at 4°C. Dishes were rinsed 3 times with 25mM PBS and treated with a mixture of PBS and 0.5% BSA for 1 hr at room temperature. Before immunopanning cells, antibody treated dishes were washed with PBS and DMEM.

OEC primary cultures were treated with 0.25% trypsin in HBSS without Ca^{2+}/Mg^{2+} for 3 mins at 37°C before trypsin inactivation with D/F medium. Cells were centrifuged at 216 g for 10 mins and resuspended in D/F medium. Cells were added to pre-treated anti-p75-NGFR dishes and incubated at 37°C for 10 mins. Unbound cells were washed off and a cell scraper was used to recover bound cells which were then subjected to a second immunopanning. Purified p75-NGFR-positive OECs were resuspended, plated on PLL-coated culture flasks, and incubated at 37°C for 7 days with medium changed every 2 days. Purified OECs were stimulated with pituitary extract (20 μg/ml, Gibco) and forskolin (2 μM, Sigma). Mitogens were removed and cells were pretreated with CellTracker™ Green CMFDA (7 μM, Molecular Probes, Eugene, OR) for 1 hr at 37°C. After rinsing, OECs were incubated with D/F medium for 1 hr, washed with PBS, and trypsinized. 100,000 OECs were added to the scar-like cultures 5–6 hours after the mechanical stretch (Fig. 1; scar-like + OEC culture).

Cerebral cortical neuron cultures

Neurons were obtained from postnatal day 6–8 rat cerebral cortices after removal of the leptomeninges. Cerebral cortices were harvested in Hibernate-A medium (BrainBits, Inc., Springfield, IL) with P/S, L-glutamine (L-glu, Gibco), and B27 supplement (Gibco), then chopped and digested with warm papain (2 mg/ml, Worthington, Lakewood, NJ) in Hibernate-A medium with P/S and L-glu. Neurons were enriched with an OptiPrep step gradient (Axis-Shield, Norton, MA). One day after stretch, all cultures received 100,000 neurons pipetted into the center of the culture (Fig. 1). After 24 hrs, cultures were fixed using 4% paraformaldehyde in Tris-buffered saline (TBS) for 1 hr and washed. Additional 24-hour co-cultures were tested for neuron viability and most neurons without processes co-localized with live uptake of propidium iodide, indicating loss of cell integrity. Four independent culture experiments were conducted and 1–3 wells per experiment were analyzed for each experimental variable.

Immunocytochemical procedures

Cultures were permeabilized with 0.3% Triton in TBS for 30 mins, blocked with 5% donkey and goat serum (Sigma) overnight, incubated with anti-GFAP (1:500, mouse or rabbit, BD

Biosciences Pharmingen, San Jose, CA; Dako, Carpinteria, CA) and rabbit anti-β3 tubulin (1:1500, Covance, Berkeley, CA) or mouse anti-fibronectin (1:500, BD Biosciences Pharmingen) overnight at 4°C. To visualize immunostaining, Cy3- and Cy5-conjugated fluorescent secondaries (1:250, 1:80, respectively; Jackson ImmunoResearch, West Grove, PA) were used. Nuclei were stained with Hoechst dye (Sigma) for 5 mins. Cultures were washed with TBS, dried, and then cover slipped onto glass slides with Fluorogel (Electron Microscopy Sciences, Hatfield, PA).

Imaging, neuron tracing, and statistical analysis

Images were obtained using a Zeiss LSM 510 confocal microscope. Approximately 16 fields from the central-most area of the stretch wells that contained GFAP-negative zones and multiple neurons were analyzed for neurite outgrowth. Peripheral areas were excluded for consistency. Neurons and their neurites were quantified and traced using the Neurolucida 7.50.4 neuron reconstruction program (MicroBrightField, Inc., Williston, VT). Individual neurite lengths and cell body details were exported to Microsoft Excel (Redmond, WA) using Neurolucida Explorer 4.50.4 (MicroBrightField, Inc., Williston, VT). Neurite processes were measured and the extent of their glial association was scored as aligned, crossing, or not associated. Additionally, neurons and neurite processes were binned based on their location in either a GFAP-positive or negative area. Neurons were counted in the GFAP-negative fibroblast zone only if neurites remained entirely within the GFAP-negative area. Neuron counts were normalized per image and reported as the sum of neurons analyzed in all 16 fields of each culture. Culture experiments were conducted in triplicate or quadruplicate and data sets presented as a mean ± SEM. Statistical analyses of differences between means was calculated using a two-way ANOVA, performed with JMP Software (version 10.0.0 for Microsoft Windows, SAS Institute Inc., Cary, NC). Statistical significance was determined by $p < 0.05$.

Results

Scar-like cultures mimic key aspects of spinal cord injury

To better understand how OECs interact with injured neurons *in vivo*, we tested OECs in an *in vitro* assay that recapitulates the features of a traumatic SCI. We used a scar-like culture model composed of astrocytes challenged by meningeal fibroblasts that is then mechanically stretched to induce molecular and morphological features of reactive astrogliosis and fibroblast clustering (Fig. 1; Wanner et al., 2008). Scar-like cultures reproduce features of the inhibitory environment found near the glial scar border and the lesion core after complete spinal cord transection (Fig. 2). At one month post-SCI, stellate GFAP-positive astrocytic processes bundle together to encircle the GFAP-negative, non-neural tissue in the spinal cord injury site (Fig. 2A–B). Similarly in scar-like cultures elongated processes of GFAP-positive reactive astrocytes surround clusters of fibronectin-labeled meningeal fibroblasts (Fig. 2E). Thus borders are established separating the astrocyte and fibroblast areas similar to those found after SCI (Fig. 2C–E; Göritz et al., 2011; Reier and Houle, 1988; Wanner et al., 2008, 2013). Neurites typically avoided growing into the non-permissive GFAP-negative fibroblast areas (Fig. 2C). Therefore, our scar-like cultures

provide multiple small-scale zones of astrocytic scar borders reminiscent of the inhibitory scar border formed following SCI.

Features of reactive astrogliosis and GFAP immunoreactivity remained following the addition of OECs to the scar-like cultures (Fig. 2C–D). OECs intermingled with astrocytes, and interestingly, they crossed the reactive astrocyte borders, and often entered into the fibroblast-filled, GFAP-negative areas (Fig. 2D–E). Neurons grown in scar-like + OEC cultures adhered and extended neurites into the non-permissive fibroblast territory primarily when they associated with OECs (Fig. 2D). These cultures, therefore, are suitable to assess if OECs can stimulate neurite outgrowth in a scar-like environment.

OECs promote neurite outgrowth in scar-like cultures

To evaluate the extent to which OECs promoted neurite outgrowth in growth-inhibitory scar-like cultures, we compared neurite outgrowth on quiescent astrocytes (positive control), and on injured astrocyte-meningeal fibroblast co-cultures in the absence or presence of OECs (scar-like or scar-like + OEC). Approximately 5,300 neurons were traced and reconstructed and the lengths of 12,700 neurites were quantified. The same percentage of neurons initiated neurite outgrowth in the three culture conditions (control 85±0.01% of neurons; scar-like 85±0.02%; scar-like + OEC 85±0.02%; mean ± SEM; n=4). Additionally, no differences were found in the mean number of neurons with neurites sampled per culture (control 117±16 neurons; scar-like 135±20; scar-like + OEC 135±17; n=4). Likewise, the number of neurons that failed to grow any neurites did not differ between cultures. These neurons were excluded from further analysis as more than 90% co-localized with propidium iodide.

Postnatal cerebral cortical neurons grew long, branching neurites over control quiescent astrocyte lawns, while neurons on reactive astrocytes in scar-like cultures had short unbranched processes (Fig. 3A, B). When OECs were added to scar-like cultures, neurite outgrowth was restored to levels closer to control cultures (compare Fig. 3C to 3A) and these long neurites commonly were associated with OECs (Fig. 3D). Total neurite tree lengths of neurons grown on control astrocyte cultures were longer than those grown on scar-like cultures without or with OECs (Fig. 3E; control 304±26 μm; scar-like 136±17 μm; $p< 0.0001$; scar-like + OECs 217±17 μm; $p< 0.05$; n=4). The addition of OECs to the scar-like cultures increased total neurite outgrowth 60% above that measured in scar-like cultures alone (Fig. 3B–E; $p< 0.01$).

OECs enhance neurite outgrowth by neurite-OEC association

Having established the ability of OECs to promote neurite outgrowth in scar-like cultures, we next asked how OECs enhance neurite outgrowth in an inhibitory environment. To determine if there was a contact-mediated effect between OEC processes and neurites, scar-like + OEC cultures were examined in confocal images. Each neurite-OEC interaction was scored into one of three categories: 1) neurites aligned with and extensively contacting an OEC process (Fig. 4A1; Align), 2) neurites that crossed an OEC process (Fig. 4A2; Cross), and 3) neurites that did not interact with OECs (Fig. 4A3; None). When single neurites were separated by association category, 52±8% of neurites aligned with OEC processes, whereas

only 23±4% (p<0.01) crossed, and 26±5% (p<0.01) never contacted OECs (Fig. 4B). Measurements of neurites aligned with OEC processes were significantly longer (Fig. 4A1, C; 135±15 μm) than those that crossed (Fig. 4A2, C; 53±9 μm; p< 0.001) or never associated with OEC processes (Fig. 4A3, C; 30±3 μm; p< 0.0001). The length of neurites that crossed OECs did not differ from those with no interaction and are combined in future analyses (p= 0.14). These data show that OECs enhanced neurite elongation through direct alignment of neuronal and OEC processes in scar-like cultures.

Fibroblast zones are more growth inhibitory than astrocyte zones

To better understand OEC-enhanced neurite outgrowth, we then characterized the effect of the two distinct cellular substrates of scar-like cultures, i.e., reactive astrocytes (Fig. 5A–B) and meningeal fibroblasts (Fig. 5C–D), on neuronal adhesion and neurite outgrowth. In scar-like cultures without OECs the percent of neurons with regenerating neurites was much greater in astrocyte than in fibroblast areas (Fig. 5E; 79±5% versus 21±5%; p<0.0001; n=3). In addition, the majority of neurites grew on astrocytes rather than on fibroblasts (Fig. 5F; 90±1% of neurites versus 10±1% of neurites; p<0.0001) and the average neurite length was nearly three times longer on astrocytes than fibroblasts (60±12 μm versus 23±5 μm; p< 0.01; n=3). The addition of OECs to the scar-like cultures increased the distribution of neurons adhering to fibroblast areas by 50% and doubled the number of neurites within those areas (Fig. 3E; 32±2% of neurons; 20±7% of neurites). Neurites also were significantly longer in astrocyte zones with, than without OECs (Fig. 5F; 92±5 μm versus 60±12 μm; p< 0.05). In fibroblast zones, however, neurite lengths in the presence or absence of OECs did not significantly differ (Fig. 5F; 41±6 μm versus 23±5 μm; p= 0.14). This suggests that fibroblasts inhibited neurite outgrowth more than reactive astrocytes and that OECs acted independent of astrocytic inhibitory factors to enhance neurite elongation.

Neurite growth aligned with OECs is enhanced on both substrates

Because OECs could enhance neurite outgrowth better in astrocyte than in fibroblast areas, we asked if this enhanced neurite outgrowth depended upon cell surface interactions between neurites and OECs. We quantified this cell surface-mediated effect by separating individual neurites into groups that aligned or did not interact with OECs and remained entirely within reactive astrocyte or fibroblast zones. On both substrates, the mean neurite length was greatest when neurites aligned with OECs compared to neurites that did not contact OECs (Fig. 5B–D, G; aligned 136±17 μm versus non-aligned 37±5 μm on astrocytes, p< 0.0001; aligned 64±12 μm versus non-aligned 20±2 μm on fibroblasts, p< 0.001). This implies that the OEC-enhanced outgrowth in fibroblast zones was previously masked when aligned and non-aligned neurite lengths were combined (Fig. 5F). We next asked if the stunted neurite outgrowth on fibroblasts in scar-like cultures (Fig. 5C, inset) could be overcome when neurites aligned to OEC surfaces (Fig. 5B, D). Neurites were nearly three times longer in fibroblast zones when they aligned with OECs compared to when they did not interact (Fig. 5G; 64±12 μm versus 23±5 μm; p< 0.01). Confocal images of neurites aligned with OECs show evidence of direct cell-to-cell contact (Fig. 5H). This shows that the inhibitory factors from fibroblasts can be overcome if the neurites are directly aligned with OECs.

Finally, to determine if neurite-OEC alignment was sufficient to enhance neurite elongation, we compared neurites that were aligned with OECs to those in quiescent astrocyte cultures and reactive astrocyte zones in scar-like cultures. When neurites aligned with OECs in reactive astrocyte zones, they were longer than neurites in quiescent or reactive astrocyte zones without OECs (Fig 5G; 136±17 μm versus quiescent astrocytes 109±7 μm, $p< 0.05$; or reactive astrocytes 60±12 μm, $p< 0.0001$). Moreover, the direct association between neurites and OEC processes in the fibroblast zones attenuated the stunted neurite outgrowth to the extent that neurite lengths matched those in the astrocyte zones of scar-like cultures (Fig. 5A, D, G; 64±12 μm versus 60±12 μm, $p< 0.78$). Together our findings support that direct cell surface alignment with OECs is required to enhance neurite elongation in both scar-like astrocyte and fibroblast environments.

Discussion

We used an established glial scar model that replicates key features of the inhibitory environment following SCI to assess if OECs enhance neurite outgrowth of postnatal cerebral cortical neurons. Analyses of neuron reconstructions showed that the presence of OECs increased the total neurite tree length of neurons grown in scar-like cultures. We identified OEC-neurite alignment as a novel method by which OECs enhanced neurite elongation. In fact, alignment with OECs more than doubled the mean neurite lengths that grew in both the astrocyte and fibroblast zones. Additionally, neurites that aligned with OECs in the scar-like astrocyte zones were significantly longer than those in permissive quiescent astrocyte areas. In combination, our data suggest that OECs provide a spatially restricted and contact-dependent growth-promoting effect on neurites that is independent of the scar-like environment.

OECs can interact with inhibitory components of the glial scar

After SCI both meningeal fibroblasts and astrocytes along the scar border act as physical and chemical barriers that disrupt regeneration (Davies et al., 1997; Pasterkamp et al., 2001; Wanner et al., 2008, 2013). Similarly, neurite outgrowth was stunted in scar-like cultures due to the scar border generated by the presence of fibroblasts and mechanical stretch (Wanner et al., 2008). Theses fibroblast and reactive astrocyte zones reportedly contain two major molecules implicated in neurite outgrowth inhibition, Sema3A and CSPGs (Pasterkamp et al., 1998, 2001; Wanner et al., 2008, 2013). Sema3A is the best known substrate-bound, growth-inhibitory factor expressed by meningeal fibroblasts *in vitro* (Niclou et al., 2003; Shearer et al., 2003) and inhibits regeneration of axons that express the Sema3A receptor neuropilin-1 (NRP-1; Pasterkamp et al., 1998, 2001). Based on studies of the developing olfactory bulb, NRP-1-positive olfactory receptor neuron axons are repelled by Sema3A, and this inhibition contributes to pre-target axon sorting between the olfactory epithelium and the olfactory bulb (Imai et al., 2009). A subset of OECs in the olfactory nerve layer express Sema3A during development and likely contribute to axon orientation during their growth into the olfactory bulb (Crandall et al., 2000; Imai et al., 2009; Schwarting et al., 2000). OECs also express NRP-1 and the down-regulation of NRP-1 expression on OECs reduces axonal outgrowth of dorsal root ganglia neurons (Roet et al., 2013). Thus, because OECs express both Sema 3A and its receptor NRP-1, they are not

repelled by meningeal fibroblasts (Fig. 2D, 5D) and therefore can influence axon orientation (Fig. 5B, D).

After SCI, astrocytes and fibroblasts up-regulate and secrete CSPGs (Bradbury et al., 2002; Burda et al., 2014; McKeon et al. 1995; Morgenstern et al. 2002). Treatment with chondroitinase ABC following injury enhances axon growth and blocks interactions between CSPGs and Sema3A to reverse the repulsive properties on neurite outgrowth (Bradbury et al., 2002; de Wit et al., 2005; Grimpe et al. 2005; McKeon et al. 1995; Zuo et al. 1998). Reportedly OECs express proteoglycanases, such as A disintegrin and metalloproteinase with thrombospondin motifs-1 and -4 (Guerout et al., 2010; Roet et al., 2013), and appear to reduce CSPG immunoreactivity in the injured spinal cord (Lakatos et al., 2003). Together with these reports our results suggest that OECs may modulate extracellular matrix components by favorably interacting with both reactive astrocytes and meningeal fibroblasts to provide a more permissive substrate and stimulate neurite regeneration.

OEC-neurite alignment stimulates outgrowth

Our quantitative findings that OEC-neuron alignment enhances neurite outgrowth on meningeal fibroblast and reactive astrocyte territories is novel, but the mechanism of their growth enhancement via cell-to-cell contact could not be addressed in this study due to the multicellular nature of the scar-like cultures. Adhesion-type molecules expressed by OECs are likely to be involved: integrins, N-cadherin, or other cell adhesion molecules (CAMs; Akins et al., 2007; Fairless et al., 2005; Miragall et al., 1988; Roet et al., 2013). OECs express L1-CAM (Runyan and Phelps, 2009; Shields et al., 2010) and are reported to support neurite outgrowth of corticospinal tract neurons (Witheford et al., 2013). L1 also modulates the response to Sema3A and associates with NRP-1 to change the Sema3A-induced chemorepulsion to chemoattraction (Castellani et al., 2000). In the olfactory bulb and nerve, OECs and olfactory receptor axons express NCAM during development and adulthood both at axon-axon and axons-OEC contacts (Miragall et al., 1988; Yoshida et al., 1999). Additionally, siRNA knockdown of OEC-expressed NCAM significantly reduced neurite outgrowth (Roet et al., 2013).

N-Cadherin regulates direct cell-to-cell adhesion and interacts with downstream signaling cascades that promote neurite outgrowth (Bixby and Zhang, 1990; Kiryushko et al., 2004). OECs express high levels of N-Cadherin yet do not appear to use it to adhere to other OECs or astrocytes (Fairless and Barnett, 2005). One possibility is that the neurites use N-Cadherin to align with OECs, in a similar manner to that demonstrated for immature Schwann cells *in vitro* (Wanner and Wood, 2002; Wanner et al., 2006). Alternatively, OECs may modulate the distribution and function of N-Cadherin via the expression of the Scavenger Receptor Class B member 2, an enhancer of regenerative sprouting (Roet et al., 2013).

OECs in this study appear to enhance neurite outgrowth in an inhibitory environment by their unique ability to enter the fibroblast zones and promote neurite alignment along their surfaces. In addition, OECs extend neurite outgrowth beyond that which growth-permissive astrocytes and reactive astrocytes are able to provide. Thus, our results provide strong

evidence that direct OEC-neurite alignment is critical to enhance neurite outgrowth in these two different inhibitory environments.

Acknowledgments

This work was supported by National Institute of Neurological Disorders and Stroke Grants 1R01NS54159 (PEP), 1R01NS076976 (PEP), 1R01NS076976a (IBW), and Christopher Reeve Paralysis Foundation WB2-060H (IBW). We thank Norianne Ingram for tracing neurites, Alyssa Capilli for the astrocyte and fibroblast zone analyses, Ana Fernandez for her advice and fibroblast image, and Dr. Aya Takeoka for OEC culture training.

Literature cited

Akins MR, Benson DL, Greer CA. Cadherin expression in the developing mouse olfactory system. J Comp Neurol. 2007; 501:483–97. [PubMed: 17278136]

Barnabé-Heider F, Göritz C, Sabelström H, Takebayashi H, Pfrieger FW, Meletis K, Frisén J. Origin of new glial cells in intact and injured adult spinal cord. Cell Stem Cell. 2010; 7:470–82. [PubMed: 20887953]

Barrett CP, Guth L, Donati EJ. Astroglial reaction in the gray matter of lumbar segments after midthoracic transection of the adult rat spinal cord. Exp Neurol. 1981; 73:365–377. [PubMed: 6167460]

Bixby JL, Zhang R. Purified N-cadherin is a potent substrate for the rapid induction of neurite outgrowth. J Cell Biol. 1990; 110:1253–60. [PubMed: 2324197]

Bradbury EJ, Moon LDF, Popat RJ, King VR, Bennett GS, Patel PN, Fawcett JW, McMahon SB. Chondroitinase ABC promotes functional recovery after spinal cord injury. Nature. 2002; 416:636–40. [PubMed: 11948352]

Burda, J.; Ao, Y.; Gao, F.; Coppola, G.; Sofroniew, M. Neuroscience 2014 Abstracts. Washington, D.C: Society for Neuroscience; 2014. Defining the astrocyte CSPG and ECM transcriptome in vivo by cell-type specific analysis of actively translated mRNA. Program No. 705.21Online

Buss A, Pech K, Kakulas BA, Martin D, Schoenen J, Noth J, Brook GA. NG2 and phosphacan are present in the astroglial scar after human traumatic spinal cord injury. BMC Neurol. 2009; 9:32. [PubMed: 19604403]

Castellani V, Chédotal A, Schachner M, Faivre-Sarrailh C, Rougon G. Analysis of the L1-deficient mouse phenotype reveals cross-talk between Sema3A and L1 signaling pathways in axonal guidance. Neuron. 2000; 27:237–49. [PubMed: 10985345]

Chandler CE, Parsons LM, Hosang M, Shooter EM. A monoclonal antibody modulates the interaction of nerve growth factor with PC12 cells. J Biol Chem. 1984; 259:6882–9. [PubMed: 6327698]

Chung RS, Woodhouse A, Fung S, Dickson TC, West AK, Vickers JC, Chuah MI. Olfactory ensheathing cells promote neurite sprouting of injured axons in vitro by direct cellular contact and secretion of soluble factors. Cell Mol Life Sci. 2004; 61:1238–45. [PubMed: 15141309]

Crandall JE, Dibble C, Butler D, Pays L, Ahmad N, Kostek C, Püschel AW, Schwarting GA. Patterning of olfactory sensory connections is mediated by extracellular matrix proteins in the nerve layer of the olfactory bulb. J Neurobiol. 2000; 45:195–206. [PubMed: 11077424]

Davies SJ, Fitch MT, Memberg SP, Hall AK, Raisman G, Silver J. Regeneration of adult axons in white matter tracts of the central nervous system. Nature. 1997; 390:680–3. [PubMed: 9414159]

De Wit J, De Winter F, Klooster J, Verhaagen J. Semaphorin 3A displays a punctate distribution on the surface of neuronal cells and interacts with proteoglycans in the extracellular matrix. Mol Cell Neurosci. 2005; 29:40–55. [PubMed: 15866045]

Doucette R. Glial influences on axonal growth in the primary olfactory system. Glia. 1990; 3:433–49. [PubMed: 2148546]

Doucette R. PNS-CNS transitional zone of the first cranial nerve. J Comp Neurol. 1991; 312:451–66. [PubMed: 1748741]

Ellis EF, McKinney JS, Willoughby KA, Liang S, Povlishock JT. A new model for rapid stretch-induced injury of cells in culture: characterization of the model using astrocytes. J Neurotrauma. 1995; 12:325–39. [PubMed: 7473807]

Fairless R, Frame MC, Barnett SC. N-cadherin differentially determines Schwann cell and olfactory ensheathing cell adhesion and migration responses upon contact with astrocytes. Mol Cell Neurosci. 2005; 28:253–63. [PubMed: 15691707]

Fitch MT, Silver J. CNS injury, glial scars, and inflammation: Inhibitory extracellular matrices and regeneration failure. Exp Neurol. 2008; 209:294–301. [PubMed: 17617407]

Göritz C, Dias DO, Tomilin N, Barbacid M, Shupliakov O, Frisén J. A pericyte origin of spinal cord scar tissue. Science. 2011; 333:238–42. [PubMed: 21737741]

Graziadei PP, Monti Graziadei GA. Neurogenesis and plasticity of the olfactory sensory neurons. Ann N Y Acad Sci. 1985; 457:127–42. [PubMed: 3913359]

Grimpe B, Pressman Y, Lupa MD, Horn KP, Bunge MB, Silver J. The role of proteoglycans in Schwann cell/astrocyte interactions and in regeneration failure at PNS/CNS interfaces. Mol Cell Neurosci. 2005; 28:18–29. [PubMed: 15607938]

Guérout N, Derambure C, Drouot L, Bon-Mardion N, Duclos C, Boyer O, Marie JP. Comparative gene expression profiling of olfactory ensheathing cells from olfactory bulb and olfactory mucosa. Glia. 2010; 58:1570–80. [PubMed: 20549746]

Hu R, Zhou J, Luo C, Lin J, Wang X, Li X, Bian X, Li Y, Wan Q, Yu Y, Feng H. Glial scar and neuroregeneration: histological, functional, and magnetic resonance imaging analysis in chronic spinal cord injury. J Neurosurg Spine. 2010; 13:169–180. [PubMed: 20672952]

Kafitz KW, Greer CA. Olfactory ensheathing cells promote neurite extension from embryonic olfactory receptor cells in vitro. Glia. 1999; 25:99–110. [PubMed: 9890625]

Kiryushko D, Berezin V, Bock E. Regulators of neurite outgrowth: role of cell adhesion molecules. Ann N Y Acad Sci. 2004; 1014:140–54. [PubMed: 15153429]

Kubasak MD, Jindrich DL, Zhong H, Takeoka A, McFarland KC, Muñoz-Quiles C, Roy RR, Edgerton VR, Ramón-Cueto A, Phelps PE. OEG implantation and step training enhance hindlimb-stepping ability in adult spinal transected rats. Brain. 2008; 131:264–276. [PubMed: 18056162]

Lakatos A, Barnett SC, Franklin RJM. Olfactory ensheathing cells induce less host astrocyte response and chondroitin sulphate proteoglycan expression than Schwann cells following transplantation into adult CNS white matter. 2003; 184:237–246.

Li Y, Li D, Raisman G. Interaction of olfactory ensheathing cells with astrocytes may be the key to repair of tract injuries in the spinal cord: the “pathway hypothesis”. J Neurocytol. 2005; 34:343–51. [PubMed: 16841171]

Li Y, Li D, Ibrahim A, Raisman G. Repair involves all three surfaces of the glial cell. Prog Brain Res. 2012; 201:199–218. [PubMed: 23186716]

Lipson AC, Widenfalk J, Lindqvist E, Ebendal T, Olson L. Neurotrophic properties of olfactory ensheathing glia. Exp Neurol. 2003; 180:167–171. [PubMed: 12684030]

López-Vales R, Forés J, Navarro X, Verdú E. Olfactory ensheathing glia graft in combination with FK506 administration promote repair after spinal cord injury. Neurobiol Dis. 2006; 24:443–54. [PubMed: 16987668]

Lu J, Féron F, Mackay-Sim A, Waite PME. Olfactory ensheathing cells promote locomotor recovery after delayed transplantation into transected spinal cord. Brain. 2002; 125:14–21. [PubMed: 11834589]

McKeon RJ, Höke A, Silver J. Injury-induced proteoglycans inhibit the potential for laminin-mediated axon growth on astrocytic scars. Exp Neurol. 1995; 136:32–43. [PubMed: 7589332]

Miragall F, Kadmon G, Husmann M, Schachner M. Expression of cell adhesion molecules in the olfactory system of the adult mouse: Presence of the embryonic form of N-CAM. Dev Biol. 1988; 129:516–531. [PubMed: 3417050]

Morgenstern DA, Asher RA, Fawcett JW. Chondroitin sulphate proteoglycans in the CNS injury response. Prog Brain Res. 2002; 137:313–32. [PubMed: 12440375]

Niclou SP, Franssen EHP, Ehlert EME, Taniguchi M, Verhaagen J. Meningeal cell-derived semaphorin 3A inhibits neurite outgrowth. Mol Cell Neurosci. 2003; 24:902–12. [PubMed: 14697657]

Pasterkamp RJ, Anderson PN, Verhaagen J. Peripheral nerve injury fails to induce growth of lesioned ascending dorsal column axons into spinal cord scar tissue expressing the axon repellent Semaphorin3A. Eur J Neurosci. 2001; 13:457–471. [PubMed: 11168552]

Pasterkamp RJ, De Winter F, Holtmaat AJ, Verhaagen J. Evidence for a role of the chemorepellent semaphorin III and its receptor neuropilin-1 in the regeneration of primary olfactory axons. J Neurosci. 1998; 18:9962–76. [PubMed: 9822752]

Pellitteri R, Spatuzza M, Russo A, Zaccheo D, Stanzani S. Olfactory ensheathing cells represent an optimal substrate for hippocampal neurons: an in vitro study. Int J Dev Neurosci. 2009; 27:453–8. [PubMed: 19446628]

Ramón-Cueto A, Valverde F. Olfactory bulb ensheathing glia: a unique cell type with axonal growth-promoting properties. Glia. 1995; 14:163–73. [PubMed: 7591028]

Ramón-Cueto A, Cordero MII, Santos-Benito FF, Avila J. Functional recovery of paraplegic rats and motor axon regeneration in their spinal cords by olfactory ensheathing glia. Neuron. 2000; 25:425–435. [PubMed: 10719896]

Ramón-Cueto A, Plant GW, Avila J, Bunge MB. Long-distance axonal regeneration in the transected adult rat spinal cord is promoted by olfactory ensheathing glia transplants. J Neurosci. 1998; 18:3803–15. [PubMed: 9570810]

Reier PJ, Houle JD. The glial scar: its bearing on axonal elongation and transplantation approaches to CNS repair. Adv Neurol. 1988; 47:87–138. [PubMed: 3278533]

Roet KCD, Franssen EHP, de Bree FM, Essing AHW, Zijlstra SJJ, Fagoe ND, Eggink HM, Eggers R, Smit AB, van Kesteren RE, Verhaagen J. A multilevel screening strategy defines a molecular fingerprint of proregenerative olfactory ensheathing cells and identifies SCARB2, a protein that improves regenerative sprouting of injured sensory spinal axons. J Neurosci. 2013; 33:11116–35. [PubMed: 23825416]

Ruitenberg MJ, Plant GW, Hamers FPT, Wortel J, Blits B, Dijkhuizen PA, Gispen WH, Boer GJ, Verhaagen J. Ex vivo adenoviral vector-mediated neurotrophin gene transfer to olfactory ensheathing glia: effects on rubrospinal tract regeneration, lesion size, and functional recovery after implantation in the injured rat spinal cord. J Neurosci. 2003; 23:7045–58. [PubMed: 12904465]

Runyan SA, Phelps PE. Mouse olfactory ensheathing glia enhance axon outgrowth on a myelin substrate in vitro. Exp Neurol. 2009; 216:95–104. [PubMed: 19100263]

Schwarting GA, Kostek C, Ahmad N, Dibble C, Pays L, Püschel AW. Semaphorin 3A is required for guidance of olfactory axons in mice. J Neurosci. 2000; 20:7691–7. [PubMed: 11027230]

Shearer MC, Niclou SP, Brown D, Asher RA, Holtmaat AJGD, Levine JM, Verhaagen J, Fawcett JW. The astrocyte/meningeal cell interface is a barrier to neurite outgrowth which can be overcome by manipulation of inhibitory molecules or axonal signalling pathways. Mol Cell Neurosci. 2003; 24:913–25. [PubMed: 14697658]

Shields SD, Moore KD, Phelps PE, Basbaum AI. Olfactory ensheathing glia express aquaporin 1. J Comp Neurol. 2010; 518:4329–41. [PubMed: 20853510]

Silver J, Miller JH. Regeneration beyond the glial scar. Nat Rev Neurosci. 2004; 5:146–56. [PubMed: 14735117]

Sofroniew MV. Molecular dissection of reactive astrogliosis and glial scar formation. Trends Neurosci. 2009; 32:638–47. [PubMed: 19782411]

Sonigra RJ, Brighton PC, Jacoby J, Hall S, Wigley CB. Adult rat olfactory nerve ensheathing cells are effective promoters of adult central nervous system neurite outgrowth in coculture. Glia. 1999; 25:256–269. [PubMed: 9932872]

Tabakow P, Raisman G, Fortuna W, Czyz M, Huber J, Li D, Szewczyk P, Okurowski S, Miedzybrodzki R, Czapiga B, Salomon B, Halon A, Li Y, Lipiec J, Kulczyk A, Jarmundowicz W. Functional regeneration of supraspinal connections in a patient with transected spinal cord following transplantation of bulbar olfactory ensheathing cells with peripheral nerve bridging. Cell Transplant. 2014; 23:1631–55. [PubMed: 25338642]

Takeoka A, Jindrich DL, Muñoz-Quiles C, Zhong H, van den Brand R, Pham DL, Ziegler MD, Ramón-Cueto A, Roy RR, Edgerton VR, Phelps PE. Axon regeneration can facilitate or suppress hindlimb function after olfactory ensheathing glia transplantation. J Neurosci. 2011; 31:4298–4310. [PubMed: 21411671]

Wanner IB. An in vitro trauma model to study rodent and human astrocyte reactivity. Methods Mol Biol. 2012; 814:189–219. [PubMed: 22144309]

Wanner IB, Anderson MA, Song B, Levine J, Fernandez A, Gray-Thompson Z, Ao Y, Sofroniew MV. Glial scar borders are formed by newly proliferated, elongated astrocytes that interact to corral inflammatory and fibrotic cells via STAT3-dependent mechanisms after spinal cord injury. J Neurosci. 2013; 33:12870–86. [PubMed: 23904622]

Wanner IB, Deik A, Torres M, Rosendahl A, Neary JT, Lemmon VP, Bixby JL. A new in vitro model of the glial scar inhibits axon growth. Glia. 2008; 56:1691–709. [PubMed: 18618667]

Wanner IB, Guerra NK, Mahoney J, Wood PM, Mirsky R, Jessen KR. The role of glial N-cadherin in Schwann cell precursors of growing nerves. Glia. 2006; 54:439–459. [PubMed: 16886205]

Wanner IB, Wood PM. N-cadherin mediates axon-aligned process growth and cell-cell interaction in rat Schwann cells. J Neurosci. 2002; 22:4066–79. [PubMed: 12019326]

Witheford M, Westendorf K, Roskams AJ. Olfactory ensheathing cells promote corticospinal axonal outgrowth by a L1 CAM-dependent mechanism. Glia. 2013; 61:1873–89. [PubMed: 24038549]

Woodhall E, West AK, Chuah MI. Cultured olfactory ensheathing cells express nerve growth factor, brain-derived neurotrophic factor, glia cell line-derived neurotrophic factor and their receptors. Brain Res Mol Brain Res. 2001; 88:203–13. [PubMed: 11295250]

Yoshida K, Rutishauser U, Crandall JE, Schwarting GA. Polysialic acid facilitates migration of luteinizing hormone-releasing hormone neurons on vomeronasal axons. J Neurosci. 1999; 19:794–801. [PubMed: 9880599]

Ziegler MD, Hsu D, Takeoka A, Zhong H, Ramón-Cueto A, Phelps PE, Roy RR, Edgerton VR. Further evidence of olfactory ensheathing glia facilitating axonal regeneration after a complete spinal cord transection. Exp Neurol. 2011; 229:109–119. [PubMed: 21272578]

Zuo J, Neubauer D, Dyess K, Ferguson TA, Muir D. Degradation of chondroitin sulfate proteoglycan enhances the neurite-promoting potential of spinal cord tissue. Exp Neurol. 1998; 154:654–62. [PubMed: 9878200]

Highlights

- We test how OECs promote neurite outgrowth in an inhibitory scar-like culture model.
- Fibroblast zones are more growth-inhibitory than astrocyte zones.
- Mean neurite length on reactive astrocytes is 2-fold greater when aligned with OECs.
- Neurite-OEC alignment enhanced outgrowth 3-fold on meningeal fibroblasts.
- OECs have a direct contact-dependent, growth-promoting effect on cortical neurites.

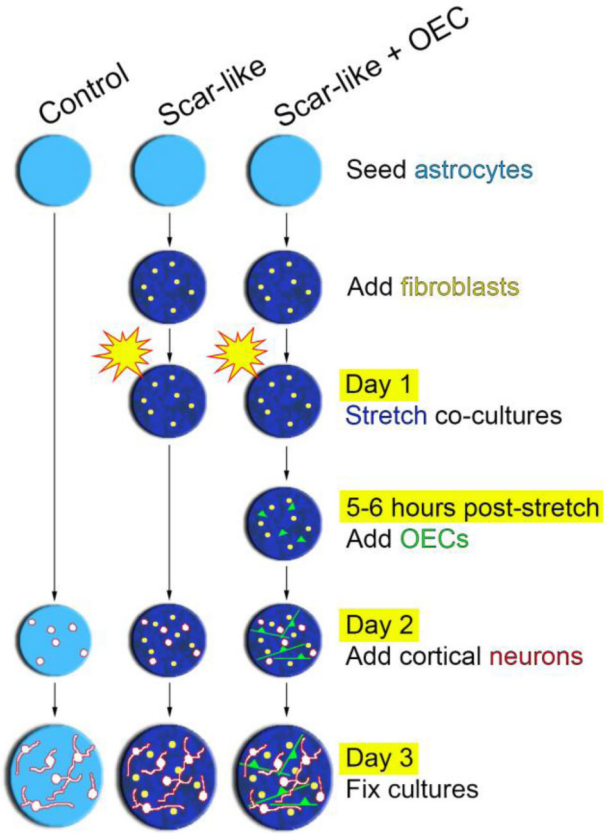

Figure 1. Schematic of experimental design and timeline

Experiments were conducted on either quiescent astrocytes (control) or co-cultures of stretched astrocytes and meningeal fibroblasts (scar-like). Mature astrocytes (light blue background) were cultured on deformable membranes and first confronted with fibroblasts to induce astrogliosis (dark blue background). Then astrocyte-fibroblast co-cultures were mechanically stretched 5–6 hours prior to the addition of OECs labeled with Cell Tracker Green (scar-like + OEC). One day later, cerebral cortical neurons (P6–P8) were added to all experimental conditions. Neurons were grown for 24 hours and fixed.

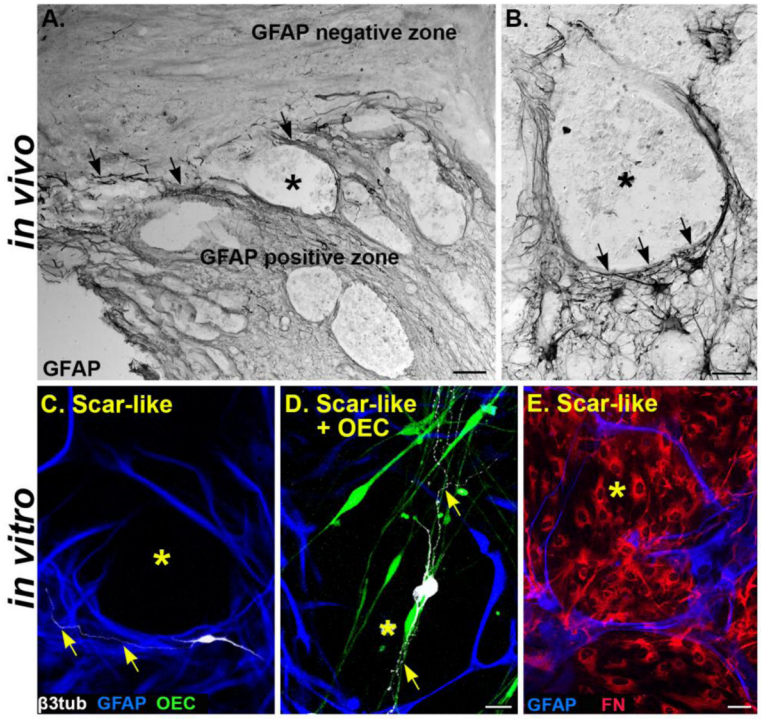

Figure 2. Scar-like cultures mimic the glial scar borders formed after spinal cord transection

(A) Lesion site from an adult rat 1 month after a complete spinal cord transection. Reactive astrocytes express high levels of GFAP at the glial scar border (black, arrows) that divides the GFAP-positive and negative zones. **(B)** A GFAP-negative lesion area (*) is surrounded by elongated GFAP-expressing astrocytic processes (black arrowheads). **(C)** Scar-like culture has GFAP-negative lesion areas (*, black) that are surrounded by GFAP-positive astrocytes (blue). Neurites (yellow arrows) from a cortical neuron (white) typically do not enter inhibitory GFAP-negative zones (*). **(D)** OECs (green) in a scar-like culture intermingle with astrocytes (blue) and span the GFAP-negative zone (*, black). Neurons (white) extend processes along the OECs (yellow arrows) in both the GFAP-positive and GFAP-negative zones. **(E)** Astrocytic processes (blue) in a scar-like culture encircle fibronectin-labeled meningeal fibroblasts (red) that are concentrated in the GFAP-negative area (*). GFAP, Glial fibrillary acidic protein; β3-tub, β3-tubulin; OEC, olfactory ensheathing cell; FN, fibronectin. Scale A= 100 μm; B, C–D, E = 50 μm.

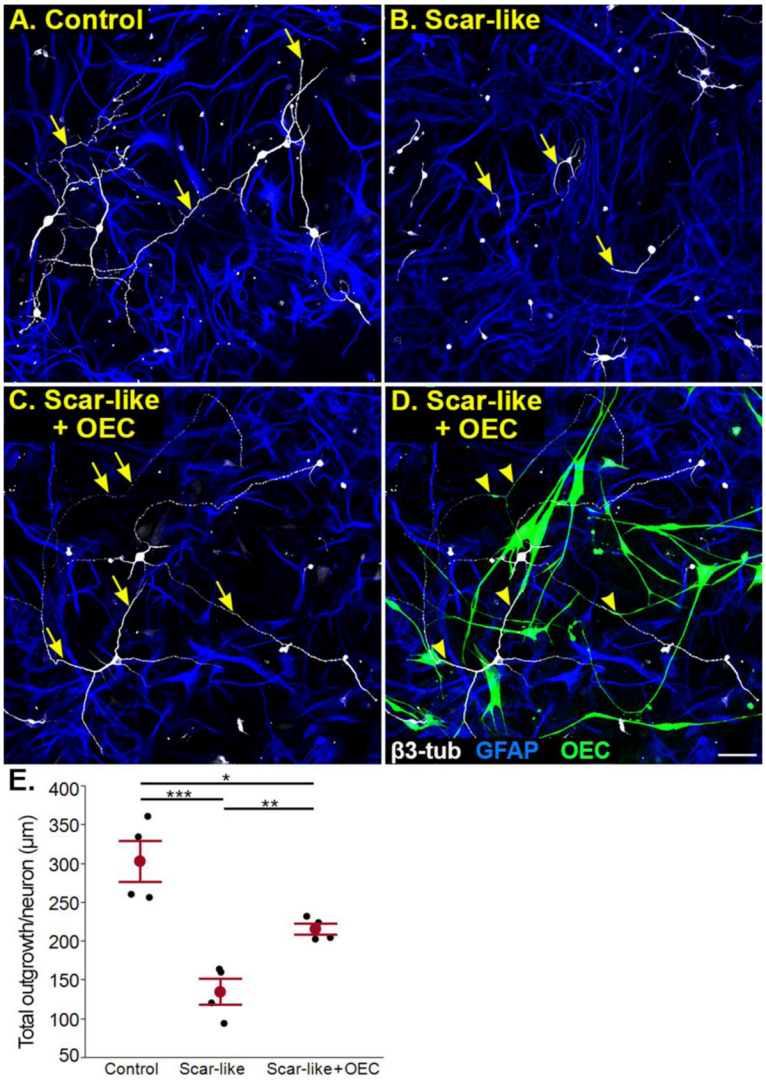

Figure 3. OECs facilitate neurite outgrowth in scar-like cultures

(A) Postnatal day 8 neurons extend long neurites (yellow arrows) on a quiescent astrocyte control culture. **(B)** A growth inhibitory scar-like culture reduces neurite extension (arrows). **(C, D)** The identical scar-like co-culture is illustrated without (C) or with OECs (D; green) to best visualize alignment of neurite outgrowth with OECs. Neurites marked by arrows in C align with OECs identified by arrowheads in D. **(E)** Average total neurite tree length per neuron in control, scar-like, and scar-like + OEC cultures. Each experiment (n=4) is represented by a black dot, while means ±SEM values for each variable are represented in red. *$p < 0.05$, **$p < 0.01$, and ***$p < 0.001$ for this and subsequent figures. GFAP, Glial fibrillary acidic protein; β3-tub, β3-tubulin; OEC, olfactory ensheathing cell. Scale A–D = 50 μm.

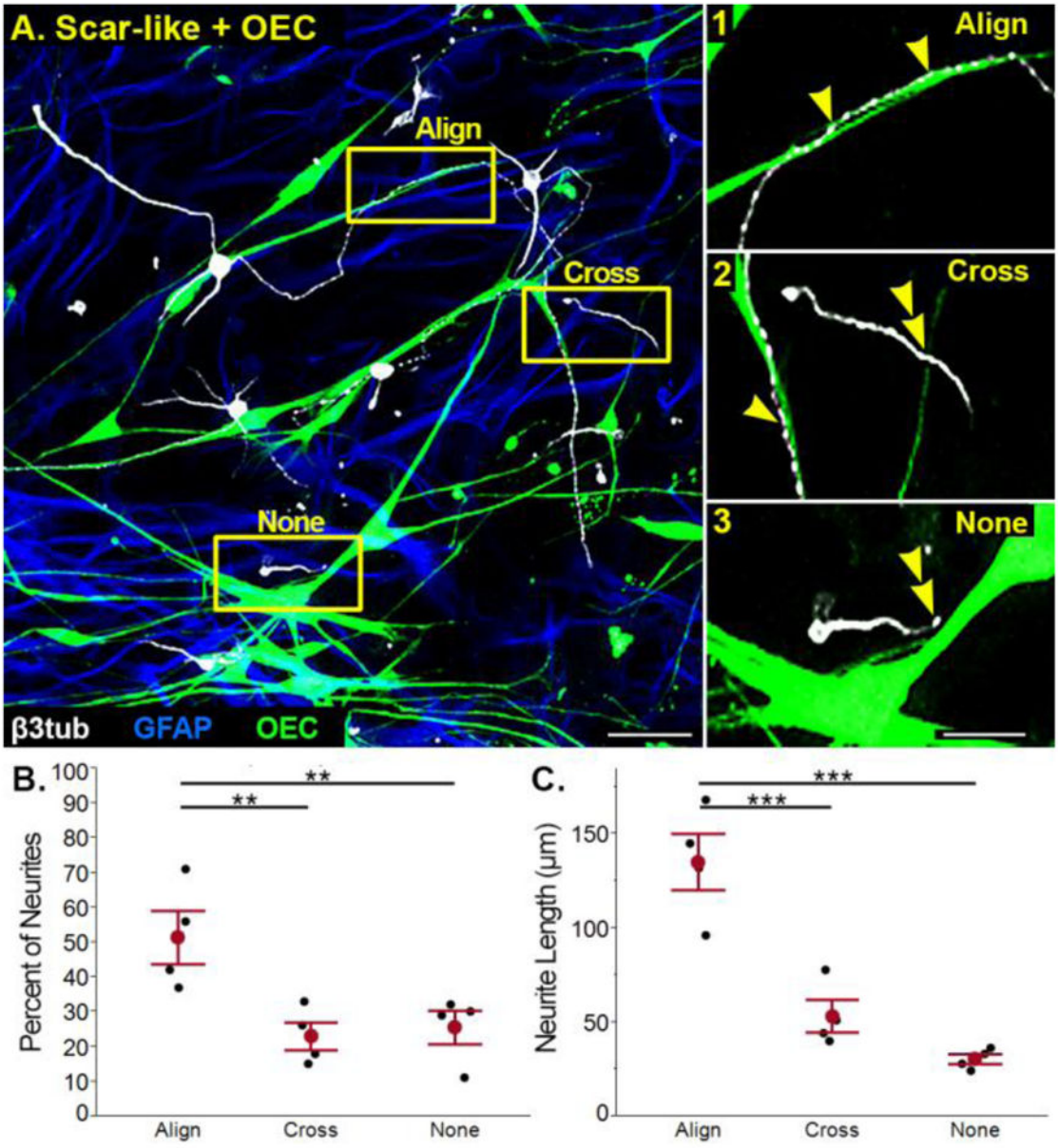

Figure 4. OEC-enhanced neurite outgrowth is mediated by neuron-OEC association

(A) In scar-like + OEC cultures associations between neurons and OECs were classified as: 1) aligned (single arrowheads), 2) crossing (double arrowhead), or 3) no interaction (double arrowhead). **(B)** An average of 52% of measured neurites aligned with OECs, while 23% of neurites crossed and 26% did not associate with OECs. **(C)** Neurites aligned with OECs were longer than those that crossed or did not associate with OECs. Individual experiments (n=4) in B and C are represented by black dots, with the means ±SEM values marked in red. GFAP, Glial fibrillary acidic protein; β3-tub, β3-tubulin; OEC, olfactory ensheathing cell. Scale A = 50 μm; A1–3 = 25 μm.

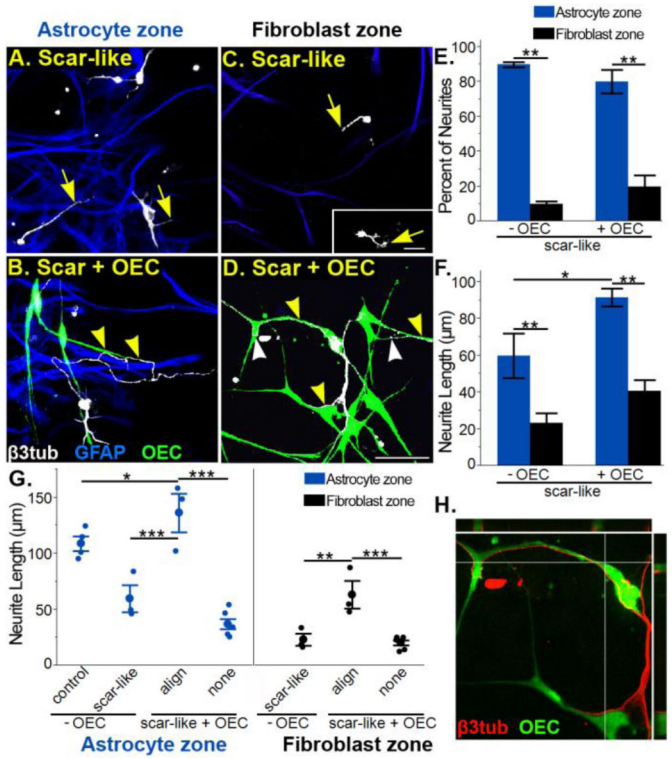

Figure 5. Neurite-OEC alignment enhances neurite outgrowth in both astrocyte and fibroblast zones

(A, C) In scar-like cultures neurons within the GFAP-positive reactive astrocyte zones (A, blue) have longer neurites (arrows) than neurons in the GFAP-negative fibroblast zones (C, black area). Retraction bulbs (arrow, inset C) are found in fibroblast areas. **(B, D)** In scar-like + OEC cultures neurons extend long processes (yellow arrowheads) within both astrocyte (B) and fibroblast zones (D) if they associate with OECs. Neurites in scar-like + OEC cultures (D) can abruptly alter their direction to maintain alignment with OECs (white arrowheads). **(E)** Quantification of the percentage of neurites that grew into astrocyte (blue) versus fibroblast (black) zones. If OECs are present, however, the percentage of neurites within the fibroblast zones doubled. **(F)** Mean neurite lengths in astrocyte (blue) versus fibroblast (black) zones show that neurites are longer in scar-like + OEC cultures in both zones than in scar-like cultures alone. **(G)** Comparison of all neurites measured and sorted by their alignment status with OECs. In both the astrocyte and fibroblast zones, neurites are significantly longer if they align with OECs (align) versus no alignment (none). Neurites that align with OECs in reactive astrocyte zones are 25% longer than neurites from quiescent astrocyte cultures alone. Neurite-OEC alignment also enhances the average neurite length in the fibroblast zones to the same level of outgrowth without OECs in the astrocyte zones. Blue (astrocyte zone) or black (fibroblast zone) dots represent neurite length averages per culture experiment (n=3) and the mean ±SEM corresponds to large dots. **(H)** Orthogonal view of direct cell-to-cell contact between an OEC (green) and neurites (red) growing exclusively in a fibroblast zone (see D). Scale A–D = 50 μm.